REGULAR ARTICLE

blood advances

The S enantiomer of 2-hydroxyglutarate increases central memory CD8 populations and improves CAR-T therapy outcome

Iosifina P. Foskolou,[1,2] Laura Barbieri,[2,3] Aude Vernet,[4] David Bargiela,[1,2] Pedro P. Cunha,[1,2] Pedro Velica,[2] Eunyeong Suh,[1] Sandra Pietsch,[1] Rugile Matuleviciute,[1] Helene Rundqvist,[2,6,7] Dominick McIntyre,[4] Ken G. C. Smith,[5] and Randall S. Johnson[1,2]

[1]Department of Physiology, Development and Neuroscience, University of Cambridge, Cambridge, United Kingdom; [2]Department of Cell and Molecular Biology (CMB), Karolinska Institutet, Solna, Sweden; [3]Department of Surgery, Oncology and Gastroenterology, University of Padua, Padua, Italy; [4]Cancer Research UK Cambridge Institute and [5]Cambridge Institute of Therapeutic Immunology and Infectious Disease, Department of Medicine, University of Cambridge, Cambridge, United Kingdom; and [6]Department of Laboratory Medicine and [7]Department of Cell and Molecular Biology, Karolinska Institutet, Huddinge, Sweden

Key Points

- S-2HG treatment maintains human CD8 T cells in a central memory state.
- CAR-T cells treated with S-2HG show superior antitumor responses.

Cancer immunotherapy is advancing rapidly and gene-modified T cells expressing chimeric antigen receptors (CARs) show particular promise. A challenge of CAR-T cell therapy is that the ex vivo–generated CAR-T cells become exhausted during expansion in culture, and do not persist when transferred back to patients. It has become clear that naive and memory CD8 T cells perform better than the total CD8 T-cell populations in CAR-T immunotherapy because of better expansion, antitumor activity, and persistence, which are necessary features for therapeutic success and prevention of disease relapse. However, memory CAR-T cells are rarely used in the clinic due to generation challenges. We previously reported that mouse CD8 T cells cultured with the S enantiomer of the immunometabolite 2-hydroxyglutarate (S-2HG) exhibit enhanced antitumor activity. Here, we show that clinical-grade human donor CAR-T cells can be generated from naive precursors after culture with S-2HG. S-2HG–treated CAR-T cells establish long-term memory cells in vivo and show superior antitumor responses when compared with CAR-T cells generated with standard clinical protocols. This study provides the basis for a phase 1 clinical trial evaluating the activity of S-2HG–treated CD19-CAR-T cells in patients with B-cell malignancies.

Introduction

Adoptive T-cell transfer (ACT) with genetically modified T cells expressing chimeric antigen receptors (CARs) has transformed cancer therapy. However, CAR-T cell exhaustion and the resultant short-term immunosurveillance limit the clinical potential of CAR-T immunotherapy.[1,2] It is well established that less-differentiated T cells, such as central memory (T_{CM}) and stem cell memory (T_{SCM}) cells, display better expansion, antitumor activity, and persistence.[3-7] However, most clinical trials use CAR-T cells generated from unsorted peripheral blood mononuclear cells (PBMCs).[8] This approach leads to inconsistent results because PBMC compositions vary among patients,[9] and the use of terminally differentiated effector cells as CAR-T products reduces antitumor responses.[10,11] Therefore, it is essential to develop new strategies for generating well-defined and persistent CAR-T products in a consistent manner.

Specific metabolites are intracellularly increased after T-cell receptor (TCR) triggering, through a mechanism that involves the hypoxia-inducible factor 1α (HIF-1α).[12,13] Although HIF-1a stabilization after TCR activation results in a metabolic switch toward glycolysis and effector differentiation,[13-15] HIF-1a is also responsible for increased concentrations of the S enantiomer of the immunometabolite 2-hydroxyglutarate (S-2HG).[12] We have previously shown that S-2HG can regulate T-cell fate in

Submitted 11 May 2020; accepted 31 July 2020; published online 17 September 2020. DOI 10.1182/bloodadvances.2020002309.

RNA-Seq data are available in the Gene Expression Omnibus database (accession number GSE155715). For original data, please contact ipf23@cam.ac.uk. Analyzed data can be found at: https://data.mendeley.com/datasets/8pp5ywc4nf/draft?a=eb53e8cb-39b0-4a5a-b6d1-2afb6bcb30de.

The full-text version of this article contains a data supplement.

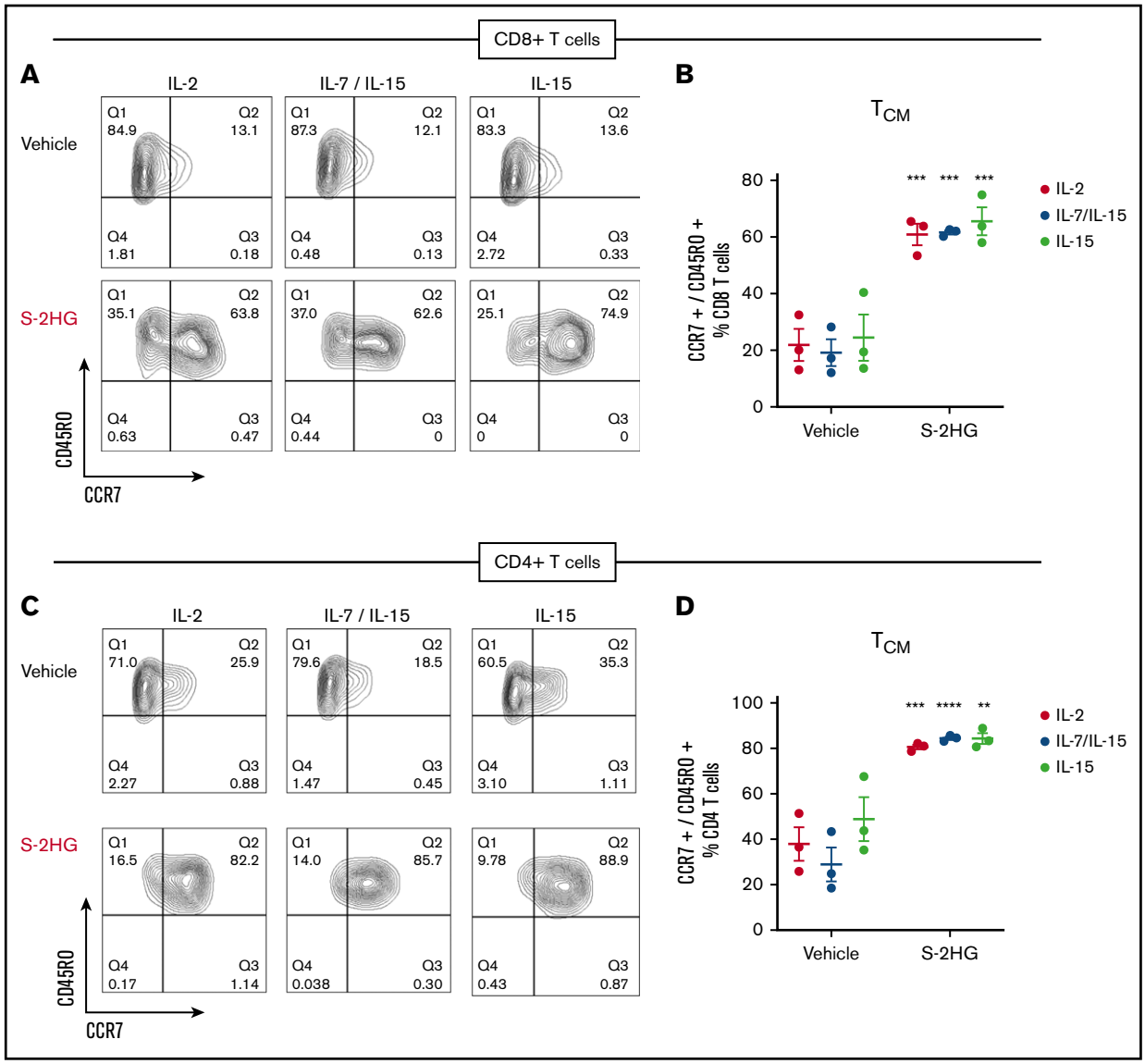

Figure 1. S-2HG treatment increases the CCR7$^+$/CD45RO$^+$ (T_{CM}) population in Pan T cells. (A) Flow cytometry plots of CD8 T cells showing surface expression of CCR7 and CD45RO following activation of pan T cells cultured with either IL-2 (30 U/mL) or IL-7/IL-15 (10 ng/mL) or IL-15 (10 ng/mL). Cells were treated with vehicle (H_2O) or S-2HG (0.6 mM) from days 0 to 8 and analyzed at day 8 by flow cytometry. Representative plots from 3 individual donors are shown. (B) Quantification of panel A. The proportion of CD8 T_{CM} (CCR7$^+$/CD45RO$^+$) cells for the different conditions is shown (mean ± standard error of the mean [SEM]). Two-way analysis of variance (ANOVA) with the Sidak multiple comparison test comparing the means of S-2HG to the means of vehicle for each culturing condition. (C) Flow cytometry plots of CD4 T cells showing surface expression of CCR7 and CD45RO following activation of pan T cells cultured with either IL-2 (30 U/mL) or IL-7/IL-15 (10 ng/mL) or IL-15 (10 ng/mL). Cells were treated with vehicle (H_2O) or S-2HG (0.6 mM) from days 0 to 8 and analyzed at day 8 by flow cytometry. Representative plots from 3 individual donors are shown. (D) Quantification of panel C. The proportion of CD4 T_{CM} (CCR7$^+$/CD45RO$^+$) cells for the different conditions is shown (mean ± SEM). Two-way ANOVA with the Sidak multiple comparison test comparing the means of S-2HG to the means of vehicle for each culturing condition. For all panels: $^{**}P \leq .01$; $^{***}P \leq .001$; $^{****}P \leq .0001$.

mouse CD8 T cells.[12] Intracellularly, S-2HG inhibits a range of a-ketoglutarate (a-KG)–dependent demethylases and hydroxylases.[16] A known S-2HG target is the ten-eleven translocation 2 (TET2) demethylase, the inhibition of which has been correlated with the production of central memory CAR-T cells and complete tumor remission in a patient.[17]

Here, we demonstrate that clinical-grade tumor-specific T_{CM} cells can be efficiently and easily generated by isolating naive CD8 T cells and complementing T-cell medium with cell-permeable S-2HG. Importantly, naive S-2HG–treated CAR-T cells show superior and long-lasting antitumor responses compared with CAR-T cells generated with protocols used in clinical trials.

Methods

Cell culture and treatments

PBMCs from healthy donors were obtained from Cambridge Bioscience or National Health Service (NHS) Blood and Transplant (NHSBT; Addenbrooke's Hospital, Cambridge, United Kingdom).

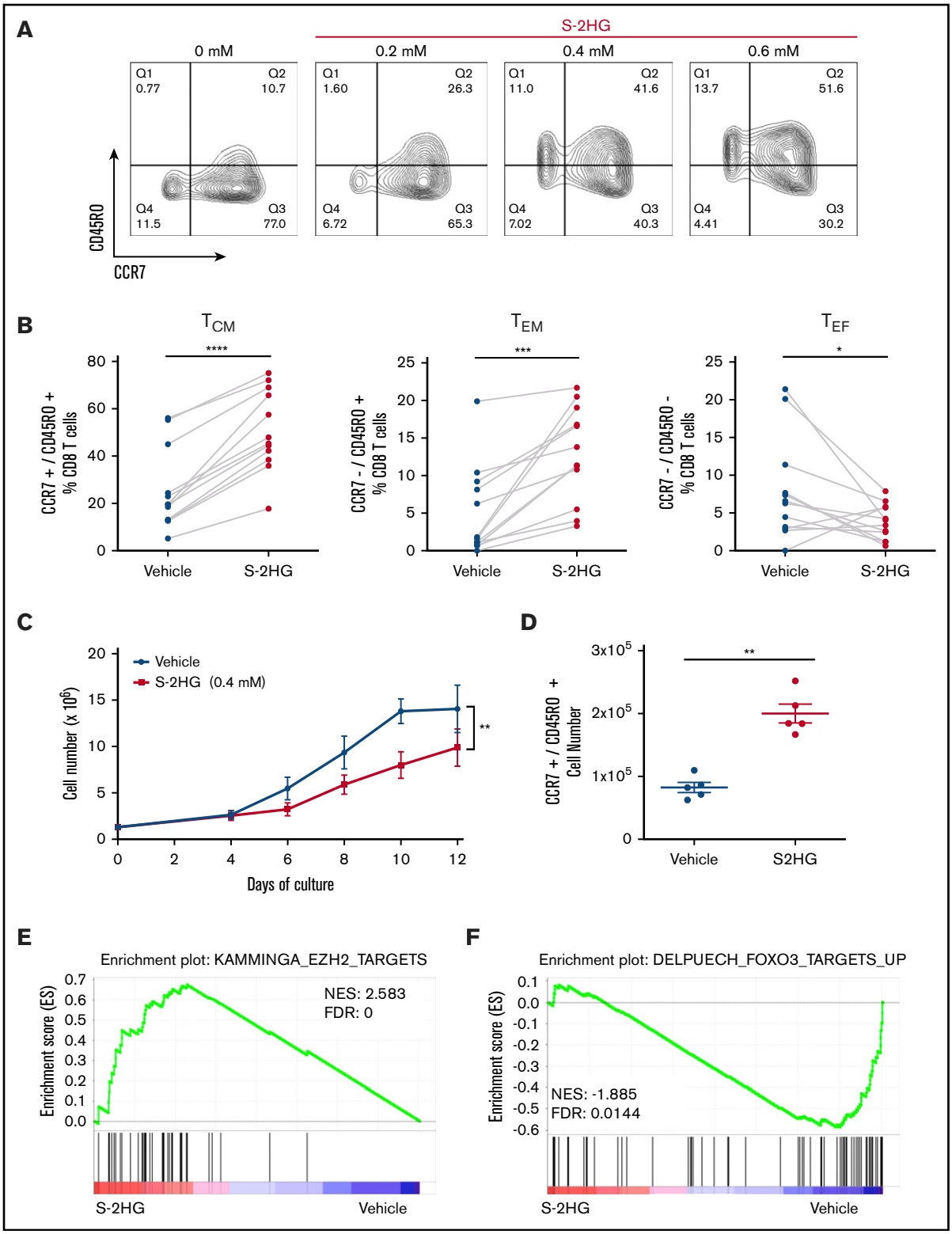

Figure 2. S-2HG treatment increases the CCR7$^+$/CD45RO$^+$ (T_{CM}) population in naive CD8 T cells. (A) Flow cytometry plots of CD8 T cells showing surface expression of CCR7 and CD45RO following activation of naive CD8 T cells cultured with IL-2 (30 U/mL). Cells were treated with vehicle (H_2O) or increasing concentrations of S-2HG from days 0 to 12 and analyzed at day 12 by flow cytometry. Representative plots of n = 5 is shown. (B) Naive CD8 T cells were isolated from 12 individual donors over 6 independent experiments. The isolated T cells were activated and treated with vehicle (H_2O) or S-2HG (0.4 mM) from days 0 to 12 and analyzed at day 12 by flow cytometry. The proportion of CD8 T_{CM} (CCR7$^+$/CD45RO$^+$), CD8 T_{EM} (CCR7$^-$/CD45RO$^+$), and CD8 T_{EF} (CCR7$^-$/CD45RO$^-$) cells is shown. Paired 2-tailed Student *t* test was used. (C) Total cell number following activation of naive CD8 T cells isolated from 5 individual donors over 3 independent experiments. Cells were activated and treated

PBMC isolation was performed within 8 to 12 hours after blood collection. T-cell isolation was performed with Miltenyi Biotec magnetic-activated cell sorting kits (Pan T cells, total $CD8^+$ T cells negative selection, and naive $CD8^+$ T cells) following manufacturer's instructions. T cells were activated with aCD3/CD28 beads (1:1 bead-to-cell ratio; Gibco) and interleukin 2 (IL-2; 30 U/mL) for 4 days. S-2HG treatment (Toronto Research Chemicals) started at day 0 (or at day 4 for CAR-T cells) and was at 0.4 mM concentration, unless stated otherwise. Every second day, fresh complete RPMI-1640 media containing IL-2 (30 U/mL) and the appropriate amount of S-2HG or vehicle was added. Cell number and viability were measured with an ADAM-MC automated cell counter (NanoEnTek) or by flow cytometry using counting beads (Invitrogen). For the Pan–T-cell experiments, cells were isolated and activated (as described earlier in this section) for 4 days in IL-2 (30 U/mL); on day 4, the activation beads were removed, and the cells were washed with phosphate-buffered saline (PBS) and divided in 3 culturing conditions (IL-2 [30 U/mL], IL-7/IL-15 [10 ng/mL], or IL-15 [10 ng/mL]). Lenti-X 293T cells were obtained from Takara; Raji-GFP-LUC and K562-LUC cells were obtained from Biocytogen. Human cells were cultured in RPMI (Gibco) or Dulbecco modified Eagle medium (DMEM; Gibco) supplemented with 10% heat inactivated fetal bovine serum (FBS; Gibco) and 1% penicillin/streptomycin (Gibco). Recombinant human IL-2 (30 U/mL; Roche) and IL-7 and/or IL-15 (10 ng/mL; BD Biosciences) were used for stimulation.

CAR-T generation

Naive or total CD8 T cells were isolated from the same donor and activated as in the previous paragraph. On day 1, lentiviral transduction was performed. Untreated tissue-culture plates were used, coated with RetroNectin (30 μg/mL; Clontech). The approximate multiplicity of infection was 100. The following lentiviral vectors purchased by Creative Biolabs were used: a truncated form of epidermal growth factor receptor (tEGFR; vector-control), anti-CD19-CAR with a 4-1BB endodomain, or an anti-CD19-CAR with a CD28 endodomain. All lentiviral constructs contained tEGFR as a surface transduction marker. After addition of the virus in each well, the plate was centrifuged at 2000*g*, at 32°C for 2 hours. After centrifugation, the supernatant was removed and the appropriate amount of CD8 T cells were added in each well. On day 4, the activation beads were removed, and the cells were cultured in the presence of S-2HG (0.4 mM) or vehicle (H_2O) until day 15. The CAR^+ cells were quantified by flow cytometry after staining with an anti-EGFR antibody.

Flow cytometry

Flow cytometry was performed on day 12, unless otherwise stated. Cells were pelleted by centrifugation and stained with antibodies in fluorescence-activated cell sorting (FACS) buffer (5% fetal bovine serum, 2 mM EDTA in PBS) at 4°C for 30 to 45 minutes. CCR7 staining was performed in RPMI-1640 media at 37°C for 20 minutes. The stained cells were finally resuspended in 1× FACS-Fix (BD Biosciences) and kept at 4°C in the dark until analysis. The samples were processed 1 to 3 days after fixation. Flow cytometers used were the BD LSR-Fortessa and AttuneX (Invitrogen). The flow data were analyzed using FlowJo.

The following antibodies were used: Live/Dead (Invitrogen); CCR7 (3D12; BD Biosciences); CD3 (HIT3a), CD8 (HIT8a), CD45RO (UCHL1), and CD62L (DREG-56) (all obtained from BioLegend); and EGFR (528; Santa Cruz Biotechnology).

RNA-sequencing and gene-set enrichment analysis

Naive CD8 T cells from 3 independent human donors were activated and treated with S-2HG (0.4 mM) or vehicle (H_2O) for 12 days, then collected and lysed with RNA Lysis Buffer RLT (Qiagen) containing (1:100) β-mercaptoethanol. Library preparation and paired-end RNA sequencing using Illumina NextSeq 500, as well as downstream data analysis, were performed by Active Motif. Sequenced reads were mapped to the genome using the STAR aligner with default settings and uniquely mapped reads were counted. Normalized counts per million and differential gene expression were determined with DESeq2.[18] Significantly differentially expressed genes were defined according to a false discovery rate (FDR) < 0.1 threshold. Hierarchical clustering of Z score and log fold-change expression values used in heatmaps was carried out using the hclust function in R version 3.6.1. RNA-Seq data are available at Gene Expression Omnibus (GEO) under accession number GSE155715.

Gene set enrichment analysis (GSEA) analysis was performed on a complete ranked list of our genes using gene sets from the Molecular Signature Database at the Broad Institute (https://www.gsea-msigdb.org/gsea/msigdb/index.jsp) as previously described.[19]

Cytotoxicity and cytokine release

Activated naive or total CD8 T cells were transduced on day 1 with an anti-CD19-CAR (4-1BB) or with tEGFR (vector-control) lentiviral construct, as described previously in "Methods." Transduced cells were treated with vehicle (H_2O) or S-2HG (0.4 mM) from days 4 to 12. On day 12, the transduced cells were cocultured with $CD19^+$ Raji-GFP^+ cells or $CD19^-$K562 cells in the stated effector/target (E:T) ratio. The cytokines were quantified by Multiplex ElectroChemical Luminescence Immunoassay (MesoScale Discovery) or by LEGENDplex (BioLegend), following the manufacturer's instructions. Cytotoxicity was assessed by FACS as: ratio of green fluorescent protein–positive (GFP^+; target)/GFP^- (reference) cells for each test coculture divided by the ratio from cultures without T cells.

Animal studies

Six- to 8-week-old female immunocompromised (NSG) mice (Charles River) were used for ACT. Mice were IV injected with 1×10^6 $CD19^+$ Raji-GFP-LUC cells on day −7. On day −1, the tumor burdens were assayed and mice with similar tumor burden were used for each condition. On day 0, mice were IV injected with

Figure 2. (continued) with vehicle (H_2O) or S-2HG (0.4 mM) from days 0 to 12. Cell number was quantified on the specified dates using the ADAM-MC automated cell counter (NanoEnTek). Graph shows mean ± SEM and a 2-way ANOVA was used, variance shown is treatment over time. (D) Naive CD8 T cells were isolated from 5 individual donors over 2 independent experiments. T cells were activated and treated with vehicle (H_2O) or S-2HG (0.4 mM) from days 0 to 12 and analyzed at day 12 by flow cytometry. The total cell number of CD8 T_{CM} ($CCR7^+$/$CD45RO^+$) cells was quantified by flow cytometry (mean ± SEM). Paired 2-tailed Student *t* test was used. (E-F) Naive CD8 T cells were isolated from 3 individual donors over 2 independent experiments, activated and treated with vehicle (H_2O) or S-2HG (0.4 mM) from days 0 to 12. The cells were collected on day 12 and RNA-Seq analysis followed. GSEA of Kamminga_EZH2_target (E) and Delpuech_ FOXO3_targets_up (F) in S-2HG–treated vs vehicle-treated CD8 T cells. Net enrichment score (NES) values and FDR are shown. For all panels: $^*P \leq .05$; $^{**}P \leq .01$; $^{***}P \leq .001$; $^{****}P \leq .0001$.

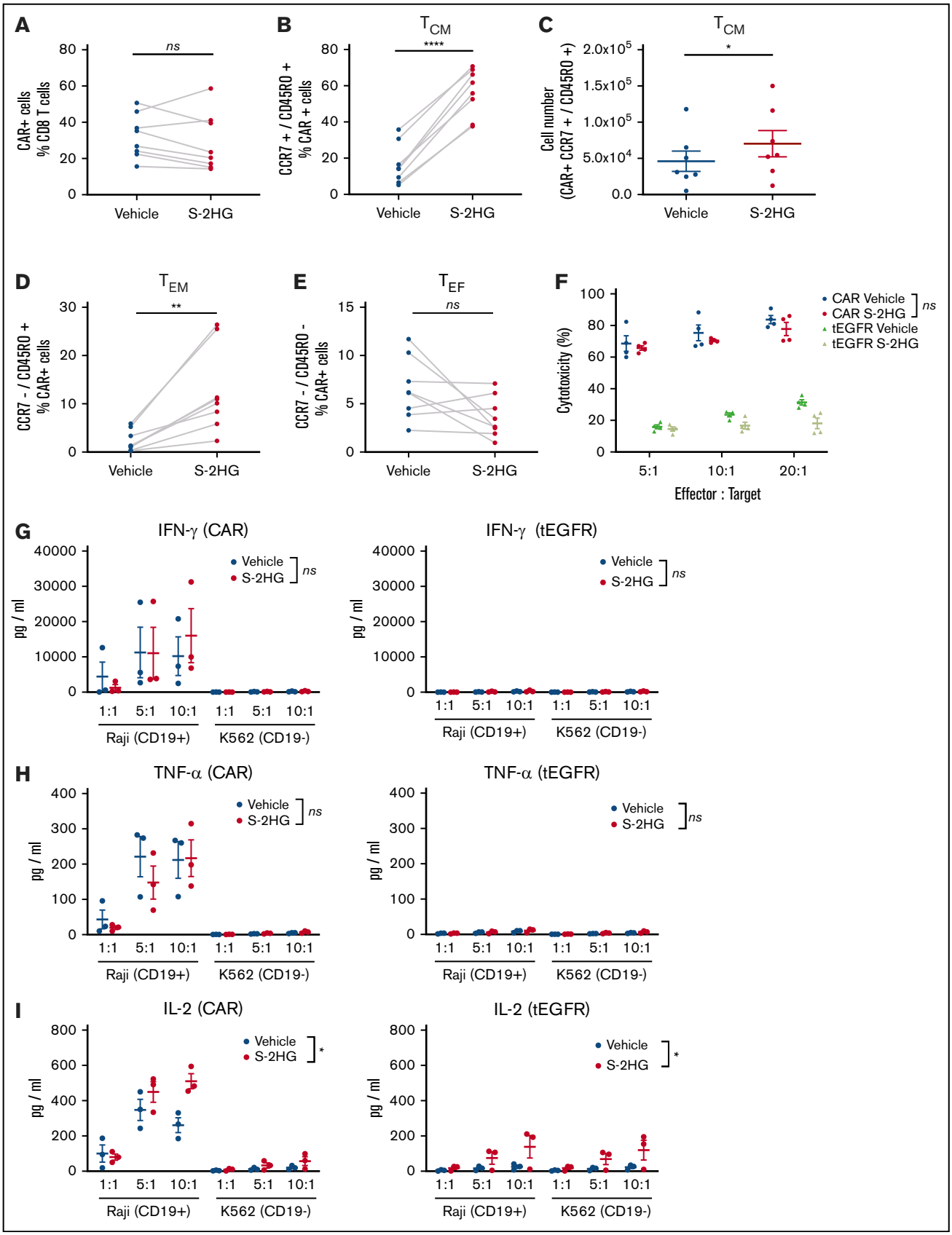

Figure 3.

2.5×10^4 CAR-T (4-1BB) cells or tEGFR T cells or PBS. The T-cell dose was based on the percentage of CAR^+ cells measured by flow cytometry 2 to 3 days before in vivo injection. The tumor burden was monitored twice a week by in vivo bioluminescent imaging with an in vivo imaging system (Xenogen IVIS 200; PerkinElmer). Before bioluminescent imaging, the mice were injected with Xenolight d-luciferin (PerkinElmer; intraperitoneal injection 10 μL/g of body weight from 15 mg/mL stock) resuspended in PBS. Both dorsal and ventral views were obtained for all animals and the tumor bulk was calculated as total flux from both images as photons per second. Mice were euthanized when they developed signs of ill health (hind-limb paralysis, loss of 15% of body weight or piloerection, and hunched posture and/or when showing very high total-flux signal $>5 \times 10^9$ photons per second). Optical imaging data analysis was carried out using Living imaging software 4.3 (PerkinElmer). Imaging, survival measurements, and data analysis were performed by a blinded operator. The animal experimental protocol was approved by the UK Home Office and was in accordance with the ethical regulations of the UK Home Office and the University of Cambridge.

Statistical analysis

Statistical analysis was performed with Prism-8 software (GraphPad). Statistical significance was set at $P < .05$.

Results

S-2HG drives human Pan-T cells toward a T_{CM} phenotype

To evaluate the effect of S-2HG on human T cells, we first isolated Pan-T (CD8 and CD4) cells from healthy donors and treated them with vehicle or S-2HG for 8 days under 3 different culturing conditions (IL-2, IL-7/IL-15, and IL-15) (Figure 1A-D). S-2HG–treated CD8 and CD4 cells showed a significant increase in the T_{CM} population ($CCR7^+/CD45RO^+$) compared to vehicle, under all culturing conditions (Figure 1B,D). It has been reported that IL-7/IL-15–supplemented media maintain T cells in a less-differentiated state compared with IL-2–supplemented media.[20] However, in studies where differences were observed in T-cell subsets between IL-2– and IL-7/IL-15–supplemented media, high concentrations of IL-2 (50-100 U/mL) were used, in comparison with our studies, where 30 U/mL IL-2 concentration was used.[20,21] High IL-2 concentrations in the culturing conditions result in increased effector phenotype and function compared with low IL-2– or IL-15–cultured cells.[21,22] We found that S-2HG's effect on the T_{CM} population was independent of the cytokines used in culture, suggesting a universal mechanism by which S-2HG favors the production of memory cells.

Naive CD8 T cells treated with S-2HG show increased memory subsets

To determine dose-dependency, we isolated naive CD8 T cells from healthy donors and treated them with different concentrations of S-2HG (Figure 2A; supplemental Figure 1). High concentrations of S-2HG lowered total T-cell numbers (supplemental Figure 1A) but cell viability was not impaired for S-2HG concentrations lower than 0.8 mM (supplemental Figure 1B). Importantly, S-2HG increased the T_{CM} population ($CCR7^+/CD45RO^+$) of CD8 T cells in a dose-dependent manner (Figure 2A; supplemental Figure 1C).

The titration experiments showed that 0.4 mM S-2HG was the concentration that best balanced phenotypic outcome and cell proliferation/viability. Isolation of naive CD8 T cells from 12 donors and treatment with 0.4 mM S-2HG increased the proportion of T_{CM} and T effector memory (T_{EM}; $CCR7^-/CD45RO^+$) cells, whereas 0.4 mM S-2HG decreased the proportion of T effector (T_{EF}; $CCR7^-/CD45RO^-$) cells (Figure 2B).

Although S-2HG treatment reduced the total proliferation of the activated cells compared to vehicle (Figure 2C), the number of S-2HG–treated cells did not reach a plateau until day 12 of culture, as opposed to vehicle-treated cells, which plateaued at day 10. Additionally, the cell number of the T_{CM} population was significantly increased after 12 days of S-2HG treatment compared to vehicle (Figure 2D). These results highlight the long proliferative potential of the S-2HG–treated cells, characteristic of memory formation.[23]

We then performed RNA sequencing (RNA-Seq) comparing activated CD8 T cells that were treated with either vehicle or S-2HG for 12 days. Analysis of the most differentially expressed genes

Figure 3. In vitro assessment of S-2HG–treated CAR-T cells. (A) Naive CD8 T cells were isolated, activated, and transduced with an anti-CD19-CAR (4-1BB) lentiviral construct on day 1. After activation, cells were treated with vehicle (H_2O) or S-2HG (0.4 mM) from days 4 to 15 and analyzed at day 15 by flow cytometry. Proportion of live CD8 CAR^+ cells is shown (n = 8 donors, 4 independent experiments). Paired 2-tailed Student *t* test was used. (B-C) Naive CD8 T cells were isolated, activated, and transduced with an anti-CD19-CAR (4-1BB) lentiviral construct on day 1. After activation, cells were treated with vehicle (H_2O) or S-2HG (0.4 mM) from days 4 to 15 and analyzed at day 15 by flow cytometry. (B) Proportion of live CD8 CAR^+ T_{CM} ($CCR7^+/CD45RO^+$) cells (n = 8 donors, 4 independent experiments). (C) The total cell number of live CD8 CAR^+ T_{CM} ($CCR7^+/CD45RO^+$) cells (n = 7 donors, 3 independent experiments; mean ± SEM). Paired 2-tailed Student *t* test was used. (D-E) Naive CD8 T cells were isolated, activated, and transduced with an anti-CD19-CAR (4-1BB) lentiviral construct on day 1. After activation, cells were treated with vehicle (H_2O) or S-2HG (0.4 mM) from days 4 to 15 and analyzed at day 15 by flow cytometry. (D) Proportion of live CD8 CAR^+ T_{EM} ($CCR7^-/CD45RO^+$) cells. (E) Proportion of live CD8 CAR^+ T_{EF} ($CCR7^-/CD45RO^-$) cells. For both panels: n = 8 donors, 4 independent experiments; paired 2-tailed Student *t* test was used. (F) Activated naive CD8 T cells were transduced on day 1 with an anti-CD19-CAR (4-1BB) or with tEGFR (vector-control) lentiviral construct. Transduced cells were treated with vehicle (H_2O) or S-2HG (0.4 mM) from days 4 to 12. On day 12, the transduced cells (total population) were cocultured with $CD19^+$ Raji-GFP^+ cells or $CD19^-$ K562 cells at an effector:target (E:T) ratio of 5:1, 10:1, and 20:1. After 24 hours, cells were analyzed by flow cytometry and cytotoxicity was quantified. Results shown are the mean ± SEM (n = 4 donors, 2 independent experiments). A 2-way ANOVA with the Tukey multiple comparison test was used; variance shown is treatment over dilution. (G-I) Activated naive CD8 T cells were transduced on day 1 with an anti-CD19-CAR (4-1BB) or with tEGFR (vector-control) lentiviral construct. Transduced cells were treated with vehicle (H_2O) or S-2HG (0.4 mM) from days 4 to 12. On day 12, the transduced cells (total population) were cocultured with $CD19^+$ Raji-GFP^+ cells or $CD19^-$ K562 cells at an E:T ratio of 1:1, 5:1, and 10:1. After 6 hours, cytokine levels in the supernatant were quantified. IFN-γ levels (G), TNF-α levels (H), and IL-2 levels (I). For panels showing tEGFR (vector-control), the *y*-axis is set at the same values as the anti-CD19-CAR panels. Results shown are the mean ± SEM (n = 3 donors, 2 independent experiments). A 2-way ANOVA with the Sidak multiple comparisons test was used; variance shown is treatment over dilution. $^*P \leq .05$; $^{**}P \leq .01$; $^{****}P \leq .0001$. ns, not significant.

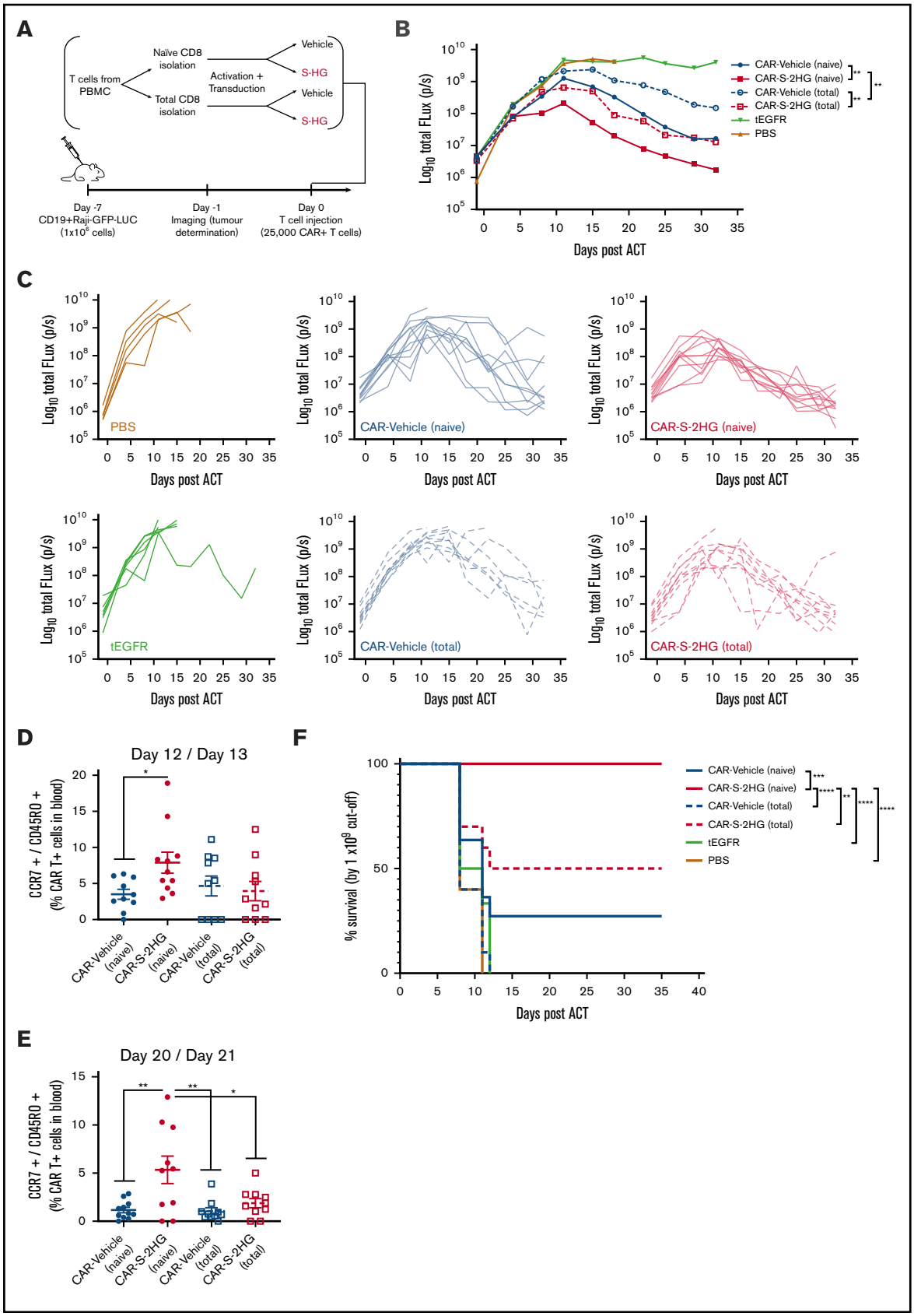

Figure 4.

showed that S-2HG–treated cells primarily increased expression of metabolism-related genes (such as *CPT1A*, *ACADVL*, *PLIN2*, and *GALM*), whereas vehicle-treated cells increased expression of adhesion- and migration-related genes (such as *TIAM1*, *XCL1*, *CXCR6*, and *SLAMF7*) (supplemental Figure 2A). S-2HG treatment increased expression of genes correlated with a T_{CM} phenotype, and decreased expression of genes correlated with STAT5 upregulation, when compared to vehicle treatment (supplemental Figure 2B-C). It has been reported that STAT5 maintains long-lived cytotoxic and effector CD8 T-cell responses.[24,25]

It is noteworthy that our RNA-Seq analysis of S-2HG– vs vehicle-treated cells showed modest differences at the messenger RNA level, suggesting alternative pathways by which S-2HG drives the observed phenotypic differences. In support of this hypothesis, GSEA of S-2HG– vs vehicle-treated cells showed enrichment in pathways implicated in messenger RNA metabolism and translational regulation (supplemental Figure 2D). Additionally, the GSEA analysis showed an enrichment of gene sets of EZH2 targets and a decrease in gene sets associated with FOXO3 targets for the S-2HG–treated cells (Figure 2E-F). EZH2 is expressed in T cells following activation, preserves hematopoietic stem cell potential, and inhibits T-cell differentiation into T_{EF} cells.[26,27] Conversely, the transcription factor FOXO3 is a crucial regulator of differentiation, and increased FOXO3 can limit the number of long-lived memory CD8 T cells.[28,29] Collectively, these results indicate that S-2HG treatment favors the accumulation of CD8 T_{CM} cells, an ideal characteristic for ACT.

S-2HG increases memory subsets in engineered CAR-T cells

To evaluate the functionality of the S-2HG–derived CD8 T_{CM} cells, we generated anti-CD19-CAR-T cells containing the 4-1BB costimulation domain by using a lentiviral construct. The transduced CD8 T cells were activated and then treated with vehicle or S-2HG for 12 to 15 days. S-2HG did not alter the transduction efficiency of CD8 T cells and there were no significant changes in the proportion of CAR^+ cells between vehicle and S-2HG (Figure 3A). Although it has been reported that CAR^+ T cells containing the 4-1BB domain drive T cells to a less-differentiated state,[30] we observed that S-2HG–treated CAR^+ CD8 T cells showed a further increase in the proportion and absolute cell number of T_{CM} and T_{EM} cells (Figure 3B-D; supplemental Figure 3A), one similar to that seen in the CD8-treated cells without the CAR construct (Figure 2B,D). A general decrease in the proportion of T_{EF} cells in CAR^+ CD8 T cells was observed, and there were no significant changes between vehicle and S-2HG treatment (Figure 3E), however, the actual cell numbers of the CAR^+ T_{EF} cells were significantly decreased after S-2HG treatment compared to vehicle (supplemental Figure 3B).

To examine whether the effect of S-2HG on CAR^+ CD8 T cells is independent of the CAR-transactivation domain, we also generated anti-CD19-CAR-T cells containing the CD28 signaling domain and treated them with S-2HG or vehicle. CD28-containing anti-CD19-CAR-T cells showed increased proportions of T_{CM} cells and decreased proportions of T_{EF} cells after S-2HG treatment (supplemental Figure 3C-E). In sum, these results demonstrate that S-2HG can increase the central memory population of CAR^+ cells independent of the transactivation domain of the CAR construct.

To assess the functionality of the CAR-T S-2HG–treated cells, we performed in vitro cytotoxicity and cytokine release assays. CD8 T cells were transduced with either anti-CD19-CAR (4-1BB) or tEGFR (vector-control) constructs, and treated with S-2HG or vehicle for 12 to 15 days. The transduced T cells were subsequently cocultured with $CD19^+$ Raji B-cell lymphoma (as target cells) and $CD19^-$ K562 myelogenous leukemia cells (as reference cells). Interestingly, although S-2HG increases the memory population of CAR^+ CD8 T cells, the immediate cytotoxic response toward target cells was not impaired compared to vehicle (Figure 3F; supplemental Figure 3F-G). Similarly, despite the general skewing in effector subsets after S-2HG treatment, there were no differences in the release of interferon γ (IFN-γ) and tumor necrosis factor α (TNF-α) between vehicle- and S-HG–treated cells (Figure 3G-H; supplemental Figure 3H). To the contrary, S-2HG treatment increased IL-2 production (Figure 3I). This observation is in agreement with our previous studies using S-2HG–treated mouse CD8 T cells.[12] High IL-2 production is another characteristic of less-differentiated $CCR7^+$ memory cells, and it has been reported

Figure 4. S-2HG–treated CAR-T cells show enhanced antitumor activity. (A) Schematic representation of the in vivo model and the different CAR-T populations used. NSG mice were injected IV with 1×10^6 Raji-GFP-LUC cells/mouse and 7 days after mice were treated with either anti-CD19-CAR-T cells or tEGFR (vector-control) T cells. Naive or total CD8 T cells were isolated from the same donor, activated, and transduced with the appropriate lentiviral construct. The anti-CD19-CAR (4-1BB) was used for CAR-T cells. After activation, cells were treated with vehicle (H_2O) or S-2HG (0.4 mM) from days 4 to 15. The NSG mice received 2.5×10^4 CAR^+ cells, or tEGFR cells or PBS. (B) Bioluminescence imaging of tumor growth of mice treated with the following conditions: CAR-Vehicle (naive); CAR-S-2HG (naive); CAR-Vehicle (total); CAR-S-2HG (total); tEGFR and PBS. The geometric mean is shown for each condition; n = 11 mice per condition for CAR-Vehicle (naive) and CAR-S-2HG (naive); n = 10 mice/condition for CAR-Vehicle (total) and CAR-S-2HG (total); n = 6 mice for tEGFR and n = 5 mice for PBS. Two independent experiments using CD8 T cells from 2 different donors. On the second experiment, the IVIS imaging on day 11 and day 32 was performed 1 day later. Statistical analysis was performed for the indicated groups by the Wilcoxon test in the $\log_{10}$ values. (C) Bioluminescence imaging of tumor growth for the individual mice per condition. Conditions shown: PBS; CAR-Vehicle (naive); CAR-S-2HG (naive); tEGFR; CAR-Vehicle (total); and CAR-S-2HG (total). Two independent experiments using CD8 T cells from 2 different donors. On the second experiment the IVIS imaging on day 11 and day 32 was performed 1 day later; n = 11 mice/condition for CAR-Vehicle (naive) and CAR-S-2HG (naive); n = 10 mice/condition for CAR-Vehicle (total) and CAR-S-2HG (total); n = 6 mice for tEGFR and n = 5 mice for PBS. (D-E) Percentage of human live CD8 CAR^+ T_{CM} ($CCR7^+$/$CD45RO^+$) cells in peripheral blood of mice 12/13 days post adoptive cell transfer (D), and 20/21 days post adoptive cell transfer (E). All conditions were compared with CAR-S-2HG (naive) with the unpaired Student *t* test; n = 10 to 11 mice/condition for CAR-Vehicle (naive) and CAR-S-2HG (naive); n = 10 mice/condition for CAR-Vehicle (total) and CAR-S-2HG (total), 2 independent experiments using CD8 T cells from 2 different donors. (F) Kaplan-Meier survival curve of Raji-GFP-LUC-bearing mice treated as in (A) and using a 1×10^9 total flux cutoff; n = 11 mice per condition for CAR-Vehicle (naive) and CAR-S-2HG (naive); n = 10 mice per condition for CAR-Vehicle (total) and CAR-S-2HG (total); n = 6 mice for tEGFR and n = 5 mice for PBS; 2 independent experiments using CD8 T cells from 2 different donors. Statistical analysis was performed using a log-rank Mantel-Cox test. For all panels: $^*P \leq .05$; $^{**}P \leq .01$; $^{***}P \leq .001$; $^{****}P \leq .0001$.

that CD8 T cells progressively lose the ability to produce IL-2 as they differentiate from naive cells to effectors.[31]

S-2HG enhances antitumor activity of CAR-T cells

We next assessed the in vivo antitumor activity of the S-2HG–treated CAR-T cells using both naive and total CD8 T cells as starting material; the latter being more typically used clinically. We performed xenografts in NSG mice by injecting 1×10^6 $CD19^+$ Raji-GFP-LUC cells, followed by injection 7 days later of 2.5×10^4 CAR^+ T cells (vehicle- or S-2HG–treated) (Figure 4A; supplemental Figure 4). Tumor progression was monitored via bioluminescent (IVIS) imaging.

S-2HG–treated CAR-T cells (both naive and total) showed better in vivo antitumor responses compared to their vehicle-treated counterparts (Figure 4B-C). Specifically, we observed a significant decrease in tumor progression in S-2HG– relative to vehicle-treated naive-generated CAR-T cells, and between S-2HG– and vehicle-treated total-generated CAR-Ts (Figure 4B). In addition, we observed that tumor progression was significantly lower when naive populations were used for CAR-T generation when compared with generation of these cells from total CD8 T cells (Figure 4B). This result is in agreement with other studies,[32-34] and demonstrates that CAR-T cells generated by a homogenous naive T-cell phenotype have an increased antitumor potential. However, it is clear by both the overlaid average tumor growths (Figure 4B) and the tumor growths shown for individual mice (Figure 4C) that S-2HG–treated naive-generated CAR-T received mice had better antitumor responses compared with all other conditions examined. Importantly, the antitumor effect of S-2HG–treated naive-generated CAR-T cells was not lost when later time points were assessed (supplemental Figure 5).

Examination of the CAR-T populations in the circulation at 12- and 20-days post-ACT showed that mice that received S-2HG–treated CAR-T cells (naive-generated) had increased proportions of CAR^+ T_{CM} population compared with the other treated conditions (Figure 4D-E). Finally, based on a 1×10^9 total flux (photon per second) cutoff (1000-fold tumor increase from baseline prior to ACT), we observed significantly increased survival in mice that received naive-generated S-2HG–treated CAR-T cells relative to all other conditions (Figure 4F).

Discussion

The high antitumor efficacy observed in these experiments, where we inject 10 to 40 times fewer CAR-T cells than the number typically used highlights the importance of CAR-T cell differentiation profiles. Clinical trials have also shown that the number of CAR-T cells used plays an important role. Generating CAR-T cells from naive precursor cells could be challenging as patients usually present low T-cell numbers with inconsistent cellular compositions at the beginning of the procedure.[6] However, recent advances in automated magnetic-bead T-cell isolation and engineering systems have shown promising results with robust and highly transduced T-cell products with strong proliferative potential.[6,35] Those systems are already using clinical-grade reagents for isolation of different T-cell populations (instead of unselected PBMCs)[6] and they could be easily adapted to use reagents similar to the ones used in this study for naive T-cell isolation.

Overall, enhancing immunologic memory is key for advancing CAR-T immunotherapy against both hematological and solid tumors,[36] and different approaches have been explored to augment long-term persistence. For example, it has been shown that ex vivo expansion of CD8 T cells with specific cytokines (such as IL-7, IL-15, and IL-21) can increase memory T-cell formation, proliferation, and survival.[20,34,37,38] In addition, T_{SCM} cells can be derived by limiting reactive oxygen species via pharmacological inhibition[4] or targeting the Wnt/β-catenin pathway[7] or using a combination of IL-7, IL-21, and a glycogen synthase-3β inhibitor[39] on naive CD8 T cells. Different costimulation domains on the CAR constructs have also been used as a strategy for increased immunologic memory.[11,30]

In our study, S-2HG was able to generate T_{CM} cells independent of the cytokines used in culture and the CAR costimulation domain, making this approach both simple and adaptable to already existing clinical protocols. In addition, because S-2HG is a naturally occurring metabolite found in healthy individuals, we believe that its presence will have few side effects and low toxicity compared with chemical inhibitors. In sum, this study demonstrates that the generation of a clinically favorable subset of CAR-T cells with propitious phenotypic and functional properties can be derived culturing naive-isolated CD8 cells with the S enantiomer form of 2HG.

Acknowledgments

The authors thank Kevin Brindle, Gemma Cronshaw, Mike Mitchell, the Cancer Research UK (CRUK) Cambridge Institute preclinical imaging core, and the staff of the CRUK Cambridge Institute Biological Resources Unit for their advice and guidance as well as expert animal care. The authors also thank the Cambridge NIHR BRC Cell Phenotyping Hub and the flow cytometry facility from the University of Cambridge School of the Biological Sciences for reagents and expert advice.

This work was supported by Apollo Therapeutics, the Knut and Alice Wallenberg Foundation Scholar Award, the Swedish Research Council (Vetenskapsrådet) and a Wellcome Trust Principal Research Fellowship award (R.S.J.), the Evelyn Trust Cambridge (Patrick Sisson's Research Fellowship) and the Karolinska Institutet (Jonas Söderquists Grant) (I.P.F.), and a Foundation for Science and Technology scholarship (SFRH/BD/115612/2016) (P.P.C.).

Authorship

Contribution: I.P.F. conceived, designed, performed, and interpreted the majority of the experiments and wrote the manuscript; L.B., A.V., D.B., P.P.C., P.V., E.S., S.P., R.M., H.R., D.M., and K.G.C.S. conducted and analyzed experiments and/or reviewed the manuscript; and R.S.J. designed the study, interpreted experiments, wrote the manuscript, and supervised the project.

Conflict-of-interest disclosure: The authors declare no competing financial interests.

ORCID profiles: I.P.F., 0000-0003-1874-6356; L.B., 0000-0001-9932-2664; P.P.C., 0000-0002-3814-6289; P.V., 0000-0002-0557-8544; S.P., 0000-0001-6398-253X; R.M., 0000-0001-5618-5700; H.R., 0000-0002-5617-9076; D.M., 0000-0002-0269-6545; K.G.C.S., 0000-0003-3829-4326; R.S.J., 0000-0002-4084-6639.

Correspondence: Randall S. Johnson, University of Cambridge, Physiology Building, Downing St, Cambridge CB23EG, United Kingdom; e-mail: rsj33@cam.ac.uk.

References

1. Porter DL, Hwang WT, Frey NV, et al. Chimeric antigen receptor T cells persist and induce sustained remissions in relapsed refractory chronic lymphocytic leukemia. *Sci Transl Med*. 2015;7(303):303ra139.
2. Park JH, Rivière I, Gonen M, et al. Long-term follow-up of CD19 CAR therapy in acute lymphoblastic leukemia. *N Engl J Med*. 2018;378(5):449-459.
3. Terakura S, Yamamoto TN, Gardner RA, Turtle CJ, Jensen MC, Riddell SR. Generation of CD19-chimeric antigen receptor modified CD8+ T cells derived from virus-specific central memory T cells. *Blood*. 2012;119(1):72-82.
4. Pilipow K, Scamardella E, Puccio S, et al. Antioxidant metabolism regulates CD8+ T memory stem cell formation and antitumor immunity. *JCI Insight*. 2018;3(18):122299.
5. Fraietta JA, Lacey SF, Orlando EJ, et al. Determinants of response and resistance to CD19 chimeric antigen receptor (CAR) T cell therapy of chronic lymphocytic leukemia. *Nat Med*. 2018;24(5):563-571.
6. Blaeschke F, Stenger D, Kaeuferle T, et al. Induction of a central memory and stem cell memory phenotype in functionally active CD4+ and CD8+ CAR T cells produced in an automated good manufacturing practice system for the treatment of CD19^{+} acute lymphoblastic leukemia. *Cancer Immunol Immunother*. 2018;67(7):1053-1066.
7. Gattinoni L, Zhong XS, Palmer DC, et al. Wnt signaling arrests effector T cell differentiation and generates CD8+ memory stem cells. *Nat Med*. 2009;15(7):808-813.
8. Kochenderfer JN, Dudley ME, Feldman SA, et al. B-cell depletion and remissions of malignancy along with cytokine-associated toxicity in a clinical trial of anti-CD19 chimeric-antigen-receptor-transduced T cells. *Blood*. 2012;119(12):2709-2720.
9. Thome JJ, Yudanin N, Ohmura Y, et al. Spatial map of human T cell compartmentalization and maintenance over decades of life. *Cell*. 2014;159(4):814-828.
10. Singh N, Perazzelli J, Grupp SA, Barrett DM. Early memory phenotypes drive T cell proliferation in patients with pediatric malignancies. *Sci Transl Med*. 2016;8(320):320ra3.
11. Feucht J, Sun J, Eyquem J, et al. Calibration of CAR activation potential directs alternative T cell fates and therapeutic potency [published correction appears in *Nat Med*. 2019;25(3):530]. *Nat Med*. 2019;25(1):82-88.
12. Tyrakis PA, Palazon A, Macias D, et al. S-2-hydroxyglutarate regulates CD8+ T-lymphocyte fate. *Nature*. 2016;540(7632):236-241.
13. Doedens AL, Phan AT, Stradner MH, et al. Hypoxia-inducible factors enhance the effector responses of CD8(+) T cells to persistent antigen. *Nat Immunol*. 2013;14(11):1173-1182.
14. Palazon A, Tyrakis PA, Macias D, et al. An HIF-1alpha/VEGF-A axis in cytotoxic T cells regulates tumor progression. *Cancer Cell*. 2017;32(5):669-683.e5.
15. Phan AT, Doedens AL, Palazon A, et al. Constitutive glycolytic metabolism supports CD8+ T cell effector memory differentiation during viral infection. *Immunity*. 2016;45(5):1024-1037.
16. Xu W, Yang H, Liu Y, et al. Oncometabolite 2-hydroxyglutarate is a competitive inhibitor of α-ketoglutarate-dependent dioxygenases. *Cancer Cell*. 2011;19(1):17-30.
17. Fraietta JA, Nobles CL, Sammons MA, et al. Disruption of TET2 promotes the therapeutic efficacy of CD19-targeted T cells. *Nature*. 2018;558(7709):307-312.
18. Love MI, Huber W, Anders S. Moderated estimation of fold change and dispersion for RNA-seq data with DESeq2. *Genome Biol*. 2014;15(12):550.
19. Subramanian A, Tamayo P, Mootha VK, et al. Gene set enrichment analysis: a knowledge-based approach for interpreting genome-wide expression profiles. *Proc Natl Acad Sci USA*. 2005;102(43):15545-15550.
20. Xu Y, Zhang M, Ramos CA, et al. Closely related T-memory stem cells correlate with in vivo expansion of CAR.CD19-T cells and are preserved by IL-7 and IL-15. *Blood*. 2014;123(24):3750-3759.
21. Pipkin ME, Sacks JA, Cruz-Guilloty F, Lichtenheld MG, Bevan MJ, Rao A. Interleukin-2 and inflammation induce distinct transcriptional programs that promote the differentiation of effector cytolytic T cells. *Immunity*. 2010;32(1):79-90.
22. Manjunath N, Shankar P, Wan J, et al. Effector differentiation is not prerequisite for generation of memory cytotoxic T lymphocytes. *J Clin Invest*. 2001;108(6):871-878.
23. Mahnke YD, Brodie TM, Sallusto F, Roederer M, Lugli E. The who's who of T-cell differentiation: human memory T-cell subsets. *Eur J Immunol*. 2013;43(11):2797-2809.
24. Grange M, Buferne M, Verdeil G, Leserman L, Schmitt-Verhulst AM, Auphan-Anezin N. Activated STAT5 promotes long-lived cytotoxic CD8+ T cells that induce regression of autochthonous melanoma. *Cancer Res*. 2012;72(1):76-87.
25. Tripathi P, Kurtulus S, Wojciechowski S, et al. STAT5 is critical to maintain effector CD8+ T cell responses. *J Immunol*. 2010;185(4):2116-2124.
26. He S, Liu Y, Meng L, et al. Ezh2 phosphorylation state determines its capacity to maintain CD8+ T memory precursors for antitumor immunity. *Nat Commun*. 2017;8(1):2125.
27. Goswami S, Apostolou I, Zhang J, et al. Modulation of EZH2 expression in T cells improves efficacy of anti-CTLA-4 therapy. *J Clin Invest*. 2018;128(9):3813-3818.
28. Tzelepis F, Joseph J, Haddad EK, et al. Intrinsic role of FoxO3a in the development of CD8+ T cell memory. *J Immunol*. 2013;190(3):1066-1075.

29. Sullivan JA, Kim EH, Plisch EH, Suresh M. FOXO3 regulates the CD8 T cell response to a chronic viral infection. *J Virol*. 2012;86(17):9025-9034.

30. Kawalekar OU, O' Connor RS, Fraietta JA, et al. Distinct signaling of coreceptors regulates specific metabolism pathways and impacts memory development in CAR T cells [published correction appears in *Immunity*. 2016;44(3):712]. *Immunity*. 2016;44(2):380-390.

31. Sallusto F, Lenig D, Förster R, Lipp M, Lanzavecchia A. Two subsets of memory T lymphocytes with distinct homing potentials and effector functions. *Nature*. 1999;401(6754):708-712.

32. Hinrichs CS, Borman ZA, Cassard L, et al. Adoptively transferred effector cells derived from naive rather than central memory CD8+ T cells mediate superior antitumor immunity. *Proc Natl Acad Sci USA*. 2009;106(41):17469-17474.

33. Nguyen HH, Kim T, Song SY, et al. Naive CD8(+) T cell derived tumor-specific cytotoxic effectors as a potential remedy for overcoming TGF-β immunosuppression in the tumor microenvironment. *Sci Rep*. 2016;6(1):28208.

34. Cieri N, Camisa B, Cocchiarella F, et al. IL-7 and IL-15 instruct the generation of human memory stem T cells from naive precursors. *Blood*. 2013;121(4):573-584.

35. Mock U, Nickolay L, Philip B, et al. Automated manufacturing of chimeric antigen receptor T cells for adoptive immunotherapy using CliniMACS prodigy. *Cytotherapy*. 2016;18(8):1002-1011.

36. Guedan S, Posey AD Jr., Shaw C, et al. Enhancing CAR T cell persistence through ICOS and 4-1BB costimulation. *JCI Insight*. 2018;3(1):e96976.

37. Alvarez-Fernández C, Escribà-Garcia L, Vidal S, Sierra J, Briones J. A short CD3/CD28 costimulation combined with IL-21 enhance the generation of human memory stem T cells for adoptive immunotherapy. *J Transl Med*. 2016;14(1):214.

38. Albrecht J, Frey M, Teschner D, et al. IL-21-treated naive CD45RA+ CD8+ T cells represent a reliable source for producing leukemia-reactive cytotoxic T lymphocytes with high proliferative potential and early differentiation phenotype. *Cancer Immunol Immunother*. 2011;60(2):235-248.

39. Sabatino M, Hu J, Sommariva M, et al. Generation of clinical-grade CD19-specific CAR-modified CD8+ memory stem cells for the treatment of human B-cell malignancies. *Blood*. 2016;128(4):519-528.